LIP-STUDENTS-23-04

Muon detection with a scintillator-PMT based setup

Pedro Copeto[1,a]

[1] *Faculdade de Ciências e Tecnologia, Universidade NOVA de Lisboa*

Project supervisor: Tomás Sousa, Prof. Daniel Galaviz, Diogo Miguel *October 10, 2023*

Abstract. In this study, we will use scintillators and PMT's to measure the angle and energy of muons that are created when primary particles from outer space interact with particles in Earth's atmosphere. We will also use a software called TOPAS to simulate these interactions. The goal is to determine the distribution of muons that reach the surface of the Earth.

KEYWORDS: Muons, Scintillator, TOPAS, Photomultiplier, PMT, Geant4, Detector, Cosmic Rays

1 Introduction

Cosmic rays, such as protons, alpha particles and heavier nuclei, are consistently bombarding the Earth, coming in different energies and angles[1]. We'll focus our work in the detection and characterization of the angle dependency and energy deposition of muons.

1.1 Angle distribution of muons

With a simple scintillation counter setup where the muon rate detection is measured and recorded for different zenith angles varying between 0º and 90º, where a zenith angle equal to 0º is the vertical axis and 90º the horizontal one, an angle dependency can be clearly seen for the detection of muons. For instance, taking the data obtained from the CosMo-Mill experiment[2], where a muon detector was rotating with a period of 24 hours, we can obtain the following graphic with the muon rate detection in function of the time in days.

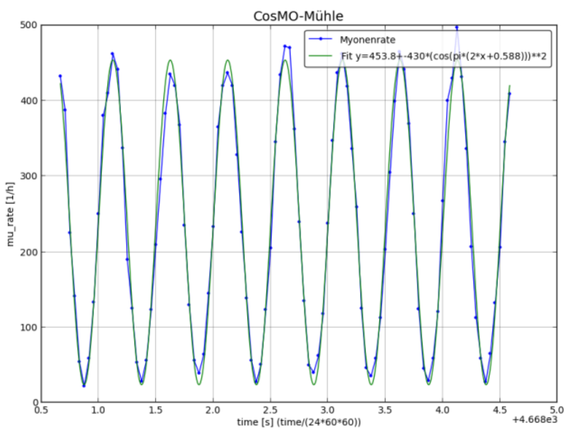

Figure 1. Investigation of the muon rates measured by the CosMO-Mill over time[2]

From the graphic of the data and it's fit function, the angle dependency of muon detection is characterized by a type of $\cos^2\theta$ function, where θ is the zenith angle.

[a] e-mail: p.copeto@campus.fct.unl.pt

1.2 Muon Energy

Since the muon detection rate is maximum for θ=0º, we'll be interested in detecting and studying muons at this angle, because this way more muons will be detected in less time than if we were to use a larger angle.

In order to determine the energy of the muons reaching our detectors, we can analyze the muon flux in the detectors in function of their momentum. Figure 2 shows this relation.

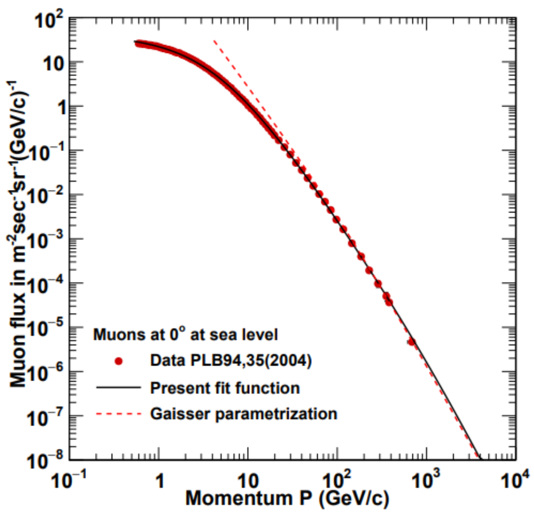

Figure 2. Muon momentum distribution with zenith angle equal to 0º, sea level.[1]

As shown from the graphic, there's a predominance of muon in the momentum range from 0.6 to 10 GeV/c. Knowing the momentum of the muon, we can calculate it's energy with:

$$E = \sqrt{p^2c^2 + m_0^2c^4} \tag{1}$$

In the momentum range referred before, we conclude that the majority of muons reach the detectors with an energy between 0.6 and 10 GeV. Furthermore, we can see that, since the mass of a muon is low, it's momentum is approximately equal to it's energy.

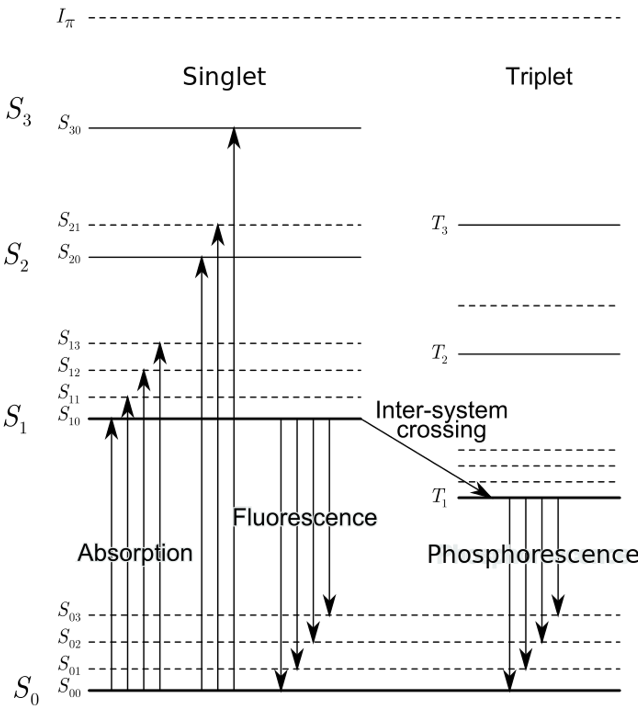

Figure 3. Energy levels of an organic molecule with π-electron structure where it can be seen different levels of absorption and corresponding levels of fluorescence[3].

1.3 Muon detectors

In order to detect muons it's usually used a setup based on scintillating detectors. Scintillators can be organic or inorganic and this are materials that have the property of, when irradiated, emitting visible light. For the particular case of organic scintillators, this process arises from transitions in the energy level structure of a single molecule. This happens when a particle, such as a muon, deposits energy in the molecules of the scintillator, leading to some of their electrons absorbing energy and being excited to higher levels of energy that then, when decaying back to their previous state, emit photons through a process of fluorescence or phosphorescence (see Figure 3).

Although muons reach the detectors with an energy between 0.6 and 10 GeV, as shown before, they only deposit a little portion of this energy while interacting with the detectors. Since muons are heavy charged particles and the ones under study are below 10 GeV, this interactions are primarily electronic and only a minor fraction (less than 1%) are radiative as we can see from the stopping power in function of the muon kinetic energy in Figure 4.

1.4 Minimum Ionizing Particle

As one can see from Figure 4, beyond the maximum, stopping power decreases approximately like $1/v^2$ with increasing particle velocity v, but after a minimum, it increases again.[5]

A minimum ionizing particle (MIP) is a particle whose mean energy loss rate through matter is close to the minimum. In many practical cases, relativistic particles, like

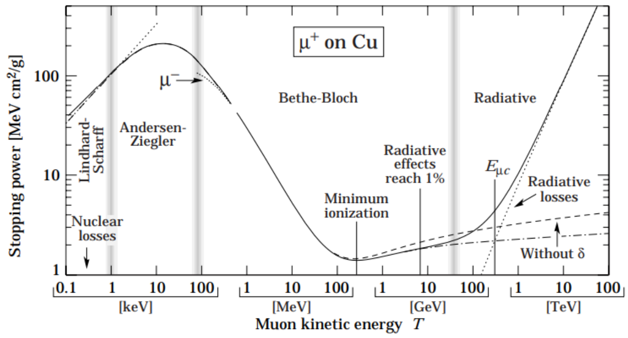

Figure 4. Stopping power ($= \langle -dE/dx \rangle$) for positive muons in copper as a function of kinetic energy T[4].

muons, are minimum ionizing particles. An important property of all minimum ionizing particles is that $\beta\gamma \simeq 3$ is approximately true where β and γ are the usual relativistic kinematic quantities. Moreover, all of the MIPs have almost the same energy loss in the material, which value is:

$$-\frac{dE}{dx} \simeq 2\frac{\text{MeV}}{gcm^{-2}} \tag{2}$$

In the case of muons, that minimum ionizing energy is equal to 1.956 MeV cm^2/g.[5]

1.5 EJ-200 Scintillators

In our setup, we'll use EJ-200 scintillators with a plane area of 253 cm^2 (see Figure5) as muon detectors. This are a kind of organic plastic scintillators that have a variety of applications and have the property of a fast response time making them favorites for beta spectroscopy and fast neutron detection, even though they have less light output comparing to inorganic scintillators. A table of properties of EJ-200 scintillators can be seen bellow:

Eljen	EJ-200
Bicron	BC-408
Scintillation Efficiency (photons/MeV)	10000
Wavelength of Max Emission (nm)	425
Decay Constant (ns)	2.1
Attenuation Length (cm)	380
Refractive Index	1.58
Density g/cm^3	1.032

*NaI(TI) is 230% on this scale

Table 1. Properties of EJ-200 Scintillator[3].

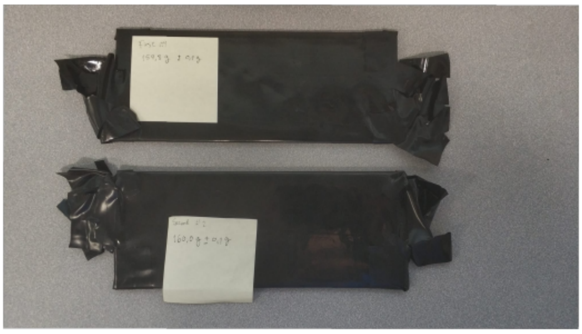

Figure 5. View of the two scintillation detectors in the simulation framework.

1.6 Dead Time

The process of fluorescence explained in the section 1.3 is associated with a certain dead time characteristic of each material. In nearly all detector systems, there will be a minimum amount of time that must separate two events in order that they be recorded as two separate pulses[3]. This time interval is known as "dead time" and it can be a problem in the detection of some particles because it prevents the detector from detecting the totality of the particles that reach it.

Muons have a frequency of 1 muon per minute per cm^2[6] for zenith=0º and this scintillators, as seen in Table 1, have a decay time of 2.1 ns. Therefore, the dead time is not a problem in our case because, since the scintillators have a plane area of 253 cm^2, in a second, about 4.2 muons reach the detector leading to a total dead time of 8.8 ns in a second. Therefore, the dead time of the scintillator in a second is just $8,8 \times 10^{-7}\%$ of that second, meaning that the probability of a muon reaching the scintillator during it's dead time is insignificant. But we also have to take in mind that there will be a dead time related to the electronic components of the experimental setup that might be significant.

1.7 Photomultiplier Tubes

Along with the scintillators, we'll use a couple of photomultiplier tubes (PMT's) mounted to each scintillator, one at each end. We use two PMT's for each scintillator instead of just one, like the majority of default detectors do, because this way we get more and better information from our detections. With the use of two PMT's we not only prevent more efficiently that the light from the scintillators doesn't gets scattered before reaching the PMT but especially we can calculate where the particle landed in our detector, which otherwise we wouldn't be able to do. We do this by measuring the difference in the time that light took to get to each of the PMT's. Doing this, and since we have to parallel scintillators with PMT's mounted on them, we can get an approximation of the trajectory that the particle took.

The use of PMT's in pair with scintillators is very common because we can not only detect a particle but also have a close approximation of the energy that the particle deposited in the detector.

A photomultiplier tube (seen in Figure 6) consists of a tube with a photocathode at one end that, when receiving light (e.g. from a scintillator), emits electrons because of the photoelectric effect. This electrons then enter a chain of dynodes charged with a certain current to create an electromagnetic field that accelerates the electrons against the dynodes, creating a sequence of electron secondary emissions, ending up multiplying the electrons that enter the tube by a large factor. The overall gain of the PMT is simply given by

$$\text{overall gain} = \alpha\delta^N \tag{3}$$

where α is the fraction of all photoelectrons collected by the multiplier structure, δ is the overall multiplication factor calculated by the coefficient between the number of secondary electrons emitted and the number of primary incident electrons and N is the number of dynodes in the structure.

All this electrons that resulted from this process then reach an anode that transforms them into an electric current proportional to the number of electrons that entered the tube and, consequently, the intensity of the light emitted by the scintillator which depends on the energy that was deposited in it by the particles.

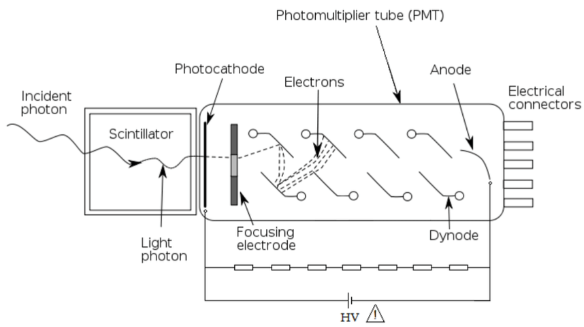

Figure 6. Photomultiplier tube (PMT).[7]

Knowing that the output current generated by the PMT is proportional to the energy deposited by the particles that reach our scintillator, we can calibrate the detector to know exactly what amount of energy was deposited depending on the output signal. Taking a naturally radioactive element that has been well studied before so that we know exactly what particles it emits and at what rate, one can use it to correlate the current it generates in the PMT with the particles it emits. Doing this for a variety of elements will lead to a good calibration of our detector.

1.8 9814B Series

In our setup, we'll use 9814B Series photomultiplier tubes from ET-Enterprises. The characteristics of this PMT can be seen in Table 2.

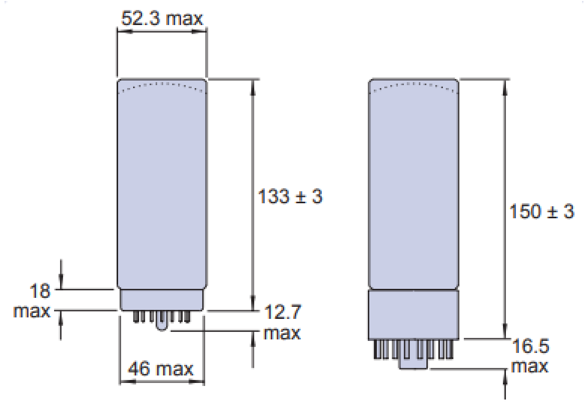

Figure 7. External dimensions of 9814B Series PMT (mm).[8]

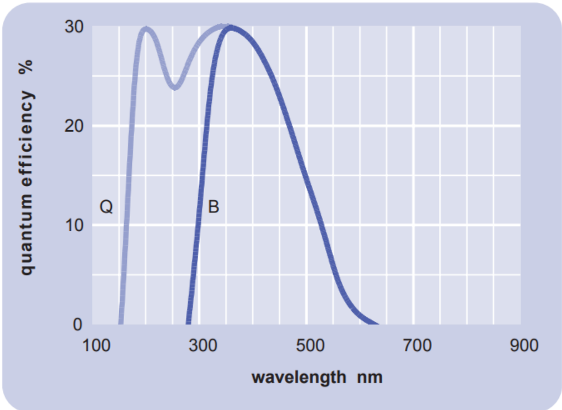

Figure 8. Typical Spectral Response Curves. From this graphic and knowing that the wavelength of max emission of our scintillators is 425 nm (Table 1), we can expect a quantum efficiency of about 26% in our setup.[8]

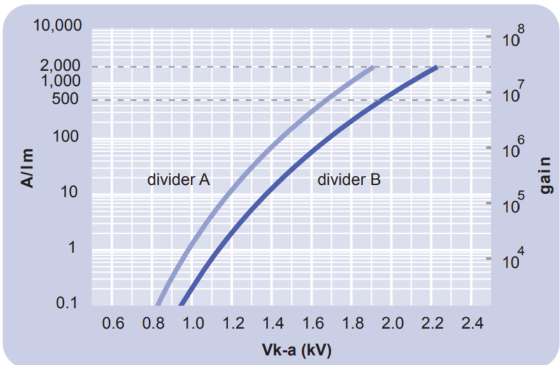

Figure 9. Typical Voltage Gain Characteristics.[8]

	unit	min	typ	max
photocathode: bialkali				
active diameter	mm		46	
quantum efficiency at peak	%		30	
luminous sensitivity	μA/lm		70	
with CB filter		8	11.5	
with CR filter			2	
dynodes: 12LFBeCu				
anode sensitivity in divider B:				
nominal anode sensitivity	A/lm		500	
max. rated anode sensitivity	A/lm		2000	
overall V for nominal A/lm	V		1950	2300
overall V for max. rated A/lm	V		2250	
gain at nominal A/lm	x10^6		7	
timing:				
single electron rise time	ns		2	
single electron fwhm	ns		3	
single electron jitter (fwhm)	ns		2.2	
transit time	ns		43	
maximum ratings:				
anode current	μA			100
cathode current	μA			100
gain	x10^6			30
sensitivity	A/lm			10000
temperature	ºC	-30		60
V (k-a)	V			2800
V (k-d1)	V			500
V (d-d)	V			450
ambient pressure (absolute)	kPa			202

Table 2. 9814B Series PMT characteristics.[8]

1.9 Quantum efficiency

The sensitivity of photocathodes can be quoted in several ways. When applied to DC light measurements, it is traditional to quote an overall photocathode efficiency in terms of current per unit light flux on its surface (amperes per lumen). A unit of greater significance in scintillation counting is the *quantum efficiency* (QE) of the photocathode. The quantum efficiency is simply defined as

$$QE = \frac{\text{number of photoelectrons emitted}}{\text{number of incident photons}} \tag{4}$$

The quantum efficiency would be 100% for an ideal photocathode, but in reality, photocathodes show maximum quantum efficiencies of 20-30%. This happens because, during the migration of electrons in the photocathode to its surface, there are electron-electron collisions but also primarily because there must be sufficient energy left for the electron to overcome the inherent potential barrier that always exists at any interface between material and vacuum. This potential barrier (often called the *work function*) is normally greater than 3 or 4 eV for most metals but can be as low as 1.5-2 eV for suitably prepared semiconductors and is responsible for the majority of electrons not escaping the photocathode[3].

2 Simulation

Before doing an experiment it is very relevant to mimic that experiment in simulation. This can provide an idea of what to expect during the experiment and what not to do. Doing so, will lead to a better optimization of an experimental setup.

2.1 TOPAS

TOPAS is a Monte Carlo tool based on Geant4 that wraps and extends it, providing an easy-to-use application. TOPAS's unique parameter control system lets you assemble and control a rich library of simulation objects (geometry components, particle sources, scorers, etc.) with no need to write C++ code[9].

In order to program the simulation, we first set the material of the *world* to "Air" and then created two geometries representing our scintillators made from the same composition and with the same dimensions of the EJ-200 scintillators.

We separated the two scintillators by 50 cm. The distance between the scintillators is important because it is an important factor for the number of particles that are detected and for the interval of angles that it detects. The bigger the distance, the less particles will be detected but the more likely each particle will come at the same angle. For example, if the two scintillators are just separated by 10 cm, as shown if Figure 10, a muon can pass through both scintillators in a range of angles from 0° to 68.4°. Making that distance equal to 50 cm, the deviation is reduced to a maximum of 26.8°.

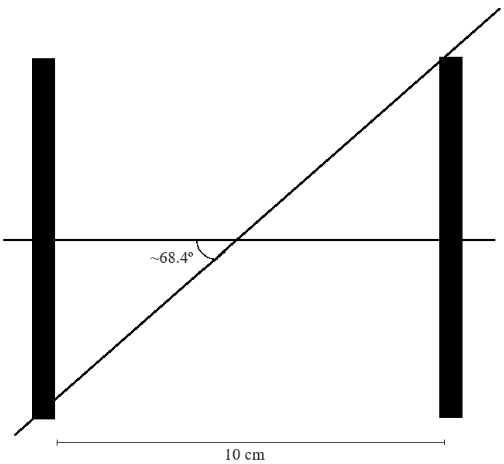

Figure 10. Scintillators separated by 10 cm. There is a deviation of -68.4° and 68.4° in the angle of the muons that are detected.

Then, we programmed our muon source with a beam shooting muons in the direction of the two scintillators with a flat energy distribution from 0.5 to 9.5 GeV and a Gaussian angular distribution with the peak representing the zenith = 0°.

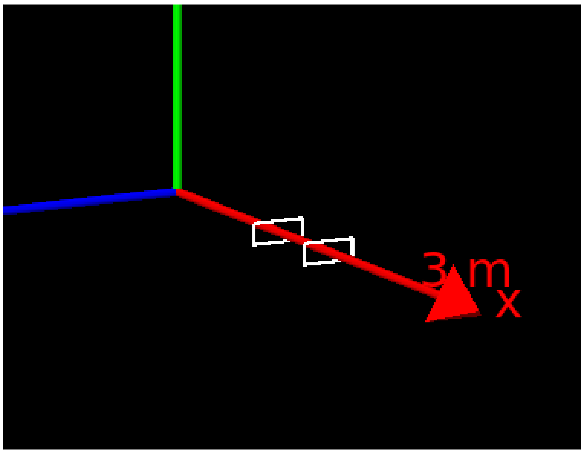

Figure 11. Scintillator setup in the simulation. The two geometries with the white outline are the scintillators.

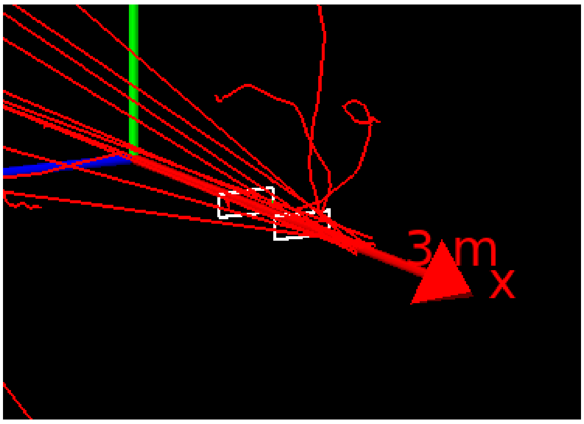

Figure 12. Simulation with 10 muons.

To retrieve measurements from our simulations, we need to program some scorers. There are two basic classes of scorers: Volume Scorers (e.g. Energy or Dose) and Surface Scorers (e.g. Track Count or Phase Space). Most scorers output overall quantities that are accumulated over many particles (counts and averages), but other scorers can output specific information per particle (in an n-tuple format)[10].

In our simulations, we had two approaches for this scorers: firstly we made an analysis using Phase Space Scorers because they give information in a much more condensed way, making any work with the data easier. Then we used the nBio Scorer that gives a lot of information about each particle in very small steps.

2.2 Phase Space Scorer

Phase Space refers to the technique of saving or replaying a set of particles crossing a given surface. By programming our phase space surfaces to be our scintillators, we can retrieve some measurements of the particles at the entry and at the exit of each scintillator. The information given by the scorers can be seen in the appendix A.1.

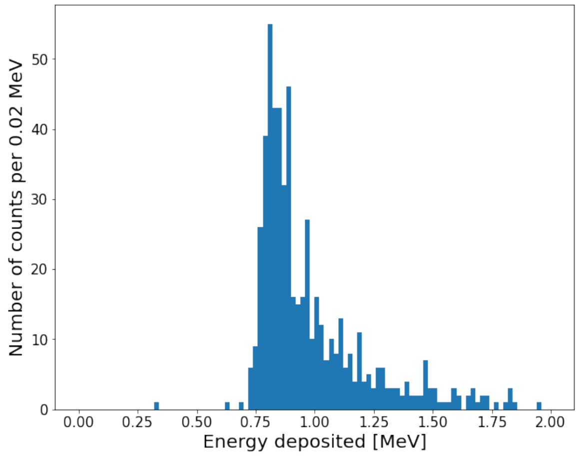

Figure 13. Distribution of the energy deposited by the muons in the scintillators for a simulation with 1000 events using the Phase Space Scorer. Here, the mean energy deposited was 1.24 MeV (as we'll see, this is significantly the highest energy average recorded. This is due to the outliers mentioned before) and the median was 0.90 MeV.

Since this scorers only give the total energy of the particle, we can approximate the energy deposited in each scintillator by making the difference between the energy at the entry of the scintillator and at the exit as the following equation shows:

$$E_{\text{entry}} - E_{\text{exit}} = E_{\text{deposited}} \tag{5}$$

This method was not always good because there's a probability that an electron is created during the passage of a muon in the scintillator leading to a significant muon loss of energy due to the creation and escaping of this electron and not to the deposition of energy in the scintillator. Because of this we had a few outliers where the energy deposited calculated was much bigger then what was expected. This led to a noticeable higher average value of the energy deposited compared to other methods coming in the next sections where there are no outliers.

In a range where the outliers are not included, the following distribution was obtained:

2.3 nBio Scorer

Using the TOPAS-nBio extension[11], we can retrieve more information from our scorers. TOPAS-nBio was developed specifically aimed at the simulation of radiobiological experiments by modeling detailed biological effects at the nanometer scale. Even though this extension is primarily aimed at a biological level, it can be very useful in the simulation of particles detection. The scorers that come with TOPAS-nBio can give a lot of information about what's happening with the particles throughout space in very short space intervals. The information given by the scorers can be seen in the appendix A.2.

With this method, we can sum all of the energy deposited by every particle in each step in the scintillator to more accurately get the distribution of the energy deposited in the scintillators, shown in Figure 14.

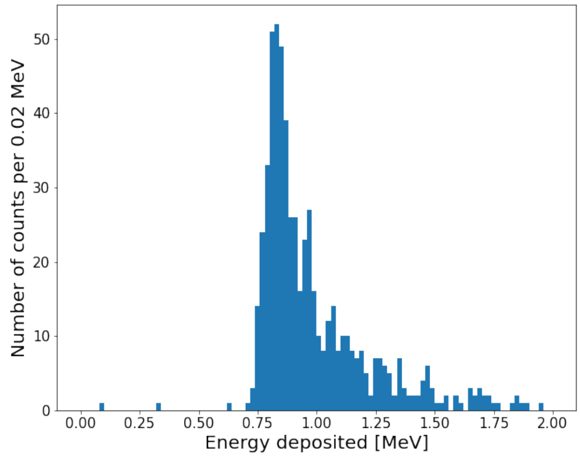

Figure 14. Distribution of the energy deposited by the muons in the scintillators for a simulation with 1000 events using the nBio Scorer. Here, the mean energy deposited was 1.01 MeV and the median was 0.90 MeV.

2.4 Cosmic-ray shower generator CRY

CRY[12] is a software that generates cosmic-ray particle shower distributions at one of three elevations (sea level, 2100 m and 11300 m) for use as input to transport and detector simulation codes. The CRY software generates a shower of cosmic particles with different energies and angles in a specified area (up to 300 m by 300 m). One can also specify the date and latitude of the simulation to get a particle shower as close as possible to reality.

In order to simulate our experiment in a more realistic way than what was done previously, we decided to change our muon source in TOPAS to a source that emitted the particles simulated in CRY. In order to do that, a script was created to translate the output given by CRY to an input that TOPAS can receive.

We simulated 500 thousand particles (muons, gammas, protons, electrons and neutrons) in a 1 m by 1 m surface at the latitude of Lisbon (38.7071) and then programmed a Phase Space source in TOPAS with the particle information given by CRY.

From our simulation, of the 500 thousand particles, only 333 passed through both scintillators, where 321 were muons and the rest electrons. Doing an analysis similar to the one done in sections 2.2 and 2.3 we obtain the distribution in Figure **??** considering all the particles that passed the two scintillators.

Discriminating the electrons and taking only the muons, we get the distribution in Figure 17.

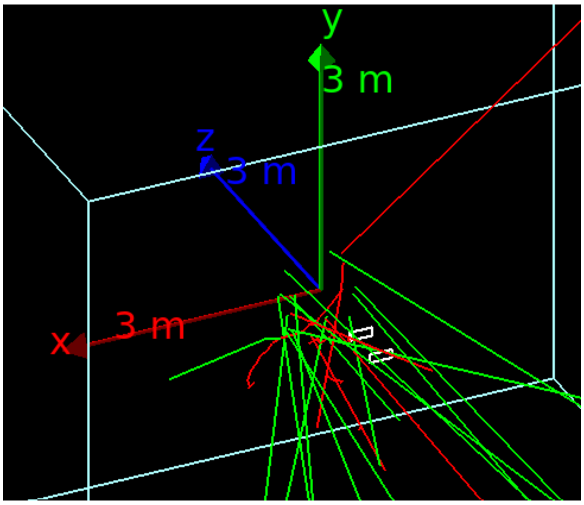

Figure 15. Example of a simulation with 20 particles given by CRY. The 1 m by 1 m particle origin surface is in the XY-plane.

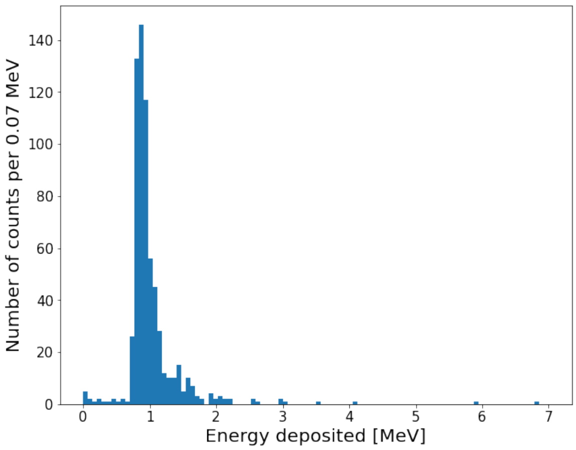

Figure 16. Distribution of the energy deposited by the particle shower given by CRY in the scintillators for a simulation with 500 thousand particles. Here, the mean energy deposited was 1.02 Mev and the median was 0.92 Mev.

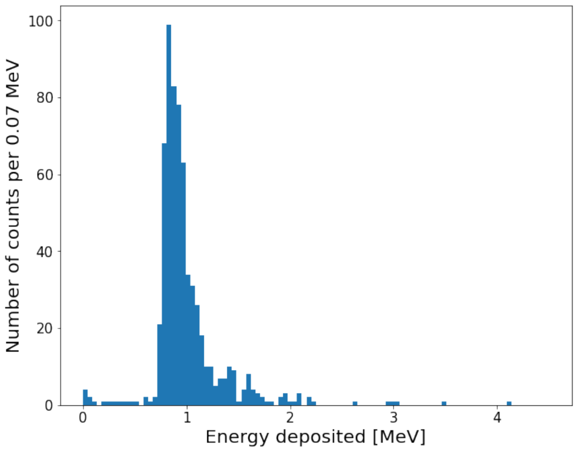

Figure 17. Distribution of the energy deposited by the muons of the particle shower given by CRY in the scintillators for a simulation with 500 thousand particles. Here, the mean energy deposited was 1.00 Mev and the median was 0.92 Mev.

2.5 Theoretical energy deposited

Assuming that the muons that are detected are minimum ionizing particles, their average stopping power is equal to S = 1.956 MeV cm^2/g as seen in section 1.4 and the density of our scintillators is ρ = 1.032 g/$cm^3$1. Knowing this, the energy deposited by the muons in the material of the scintillators can be calculated:

$$S\rho = 2.019 MeV/cm \tag{6}$$

In order to calculate the minimum energy that is deposited, it is necessary to assume that a muon passes perpendicularly into the scintillator, covering a distance equal to its width (0.52 cm in our case). Therefore, the theoretical minimum energy deposited by the muons in our scintillators is equal to 2.019 x 0.52 = 1.05 MeV. As seen from the previous plots, the simulations are giving energy deposited distributions with a mean and median values bellow the theoretical minimum energy. After changing some parameters in order to understand why that is (monoenergetic and monoangular beams, changing thickness of scintillators, changing number of steps, trying different physics lists), the problem persisted.

2.6 Geant4

In the hope of better understanding what is going on during the simulation, we took the simulations to Geant4, which is a toolkit to create simulations of the passage of particles or radiation through matter of reference. It includes a complete set of physics processes for electromagnetic, strong and weak interactions of particles in matter over a large energy range. It is used in several areas of science, from high energy, nuclear and accelerator physics, to medical and space science [13].

It includes a complete set of physics processes for electromagnetic, strong and weak interactions of particles in matter over an energy range

2.7 Energy Deposited Distribution with Geant4

Doing the same setup as before with TOPAS (see Figure 11), with two geometries representing the scintillators and a monoenergetic muon beam, we get the following energy deposited distribution:

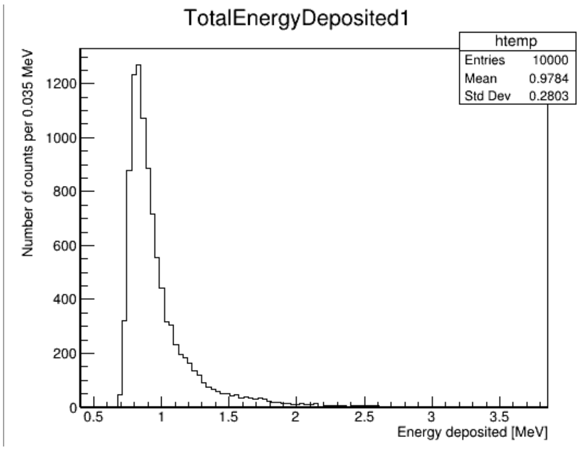

Figure 18. Distribution of the energy deposited by the muons in the first scintillator for a simulation with 10000 events. Here, the mean energy deposited was 0.978 MeV.

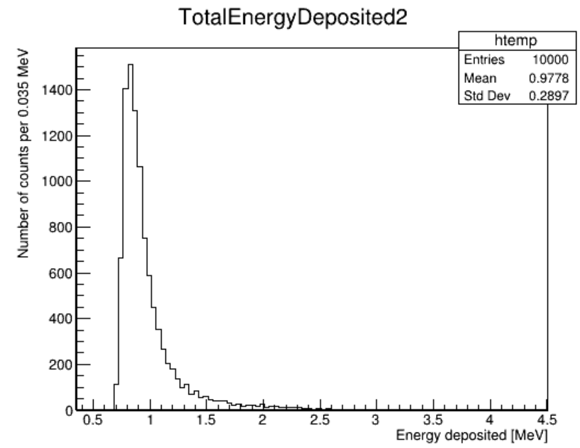

Figure 19. Distribution of the energy deposited by the muons in the second scintillator for a simulation with 10000 events. Here, the mean energy deposited was 0.978 MeV.

One can see that the mean energy deposited is still bellow the expected value got in section 2.5 for the minimum energy deposited and more work needs to be done in order to fully understand this discrepancy.

3 Experimental Setup

The final experimental setup will have two parallel scintillators with PMT's on each side. In order to place the PMT's onto the scintillators a silicone glue was made. This will be used primarily to eliminate any air between the PMT's and the scintillators, reducing the refraction of light.

Firstly, a test of this method of placing the PMT's onto the scintillators using the silicone glue was made using only one PMT glued to a scintillator in a dark box. Since this first experimental setup is only a test of this method, we did not invest much in this first setup, instead we tried, as far as we could, to use an handmade setup.

3.1 Materials

For this first test one has to have: a dark box, silicone glue, a photomultiplier tube, a scintillator, a power supply for the PMT (ORTEC 556 High Voltage Power Supply) and an oscilloscope to see the output of the PMT.

3.2 Dark box

In order to make the dark box, we used a regular card box big enough to fit the PMT and the scintillator. To make it as dark as possible, we placed black tape in every place where light entered the box. Besides that, we cut an opening on the top of the box to have access to its interior.

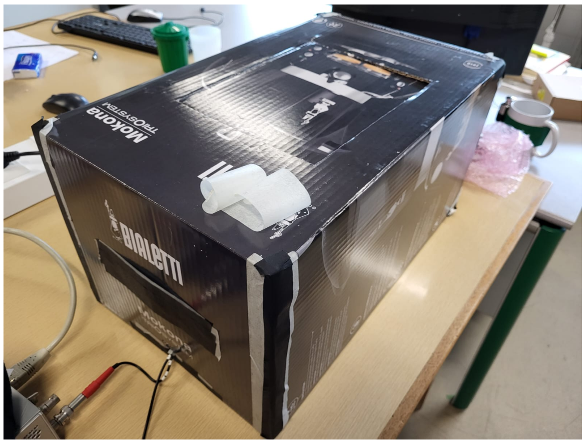

Figure 20. Card box with black tape covering the light, a hole for the PMT cables and an opening on top.

Figure 21. Card box with black tape covering the light and an opening on top.

3.3 Silicone glue

To make the silicone glue, we used UHU transparent silicone and two sheets of acrylic. The making process of the glue needs to be as clean as possible to prevent its contamination. After cleaning all the material, we placed a line of silicone in one of the acrylic sheets and then placed the other one on top to turn the silicone line into a thin layer between the two sheets. After that, we waited 24 hours for the silicone to dry with a weight on top of the acrylic sheets. Then, carefully, we separated the two acrylic sheets and retrieved the silicone layer. Finally, we used a box cutter to cut the silicone to the shape of the interception between the scintillator and the PMT.

Figure 22. Two acrylic sheets with the silicone in the middle.

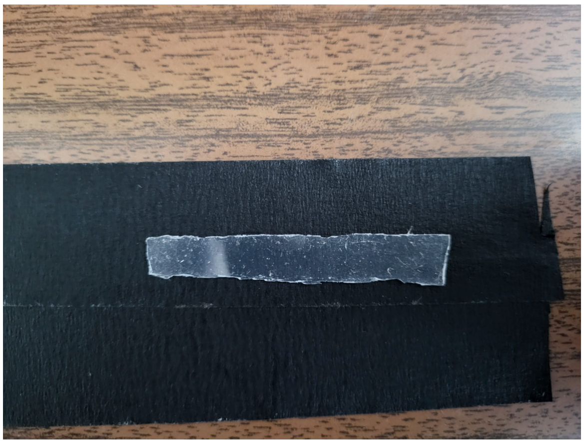

Figure 23. Example of the silicone glue after being cut.

After placing the PMT onto the scintillator with the silicone in the middle, we firmly placed the two together with black tape covering everything from light.

Figure 24. PMT placed onto the scintillator with the silicone glue on the point of contact and black tape gluing the two together and covering the materials from light.

Figure 25. PMT placed onto the scintillator with the silicone glue on the point of contact and black tape gluing the two together and covering the materials from light.

3.4 Tests

Having all the materials needed for the test, we placed the PMT and the scintillator in the dark box with a little hole for the PMT cables to come out and then supplied the PMT with 1950 V (overall V for nominal A/lm 2) and connected the output cable of the PMT in the oscilloscope.

We immediately started seeing the PMT pulses in the oscilloscope corresponding to cosmic rays entering the box and passing trough the scintillator. After this test, we can conclude that this method of placing the PMT's onto the scintillators was a success and can be used in the final setup.

Figure 26. PMT and scintillator inside the dark box.

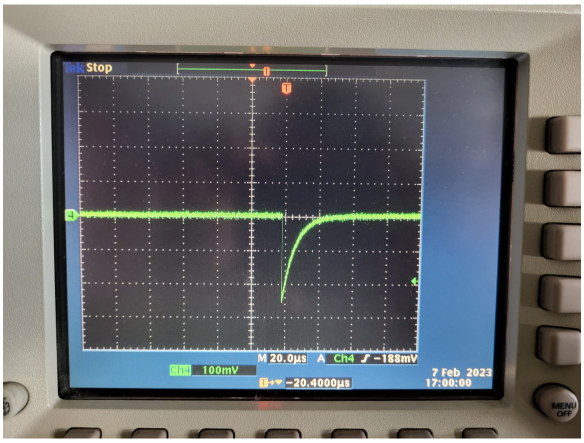

Figure 27. Example of a PMT signal in the oscilloscope.

4 Results and Conclusions

One important thing to notice in the simulation work is that, as seen in section 2.5, it was expected a theoretical minimum energy deposited of 1.05 MeV but in every simulation (except the one in section 2.2 because of the outliers) we got a mean energy deposited bellow that value which, in theory, should be impossible.

Regarding the experimental setup, we can be confident that the silicone glue is a good method and now, for the future, we'll work on a better setup with a good dark box and with the two scintillators in parallel with a PMT on each side of them.

Acknowledgements

I would like to sincerely thank all of the NUC-RIA team and particularly my supervisor Tomás Sousa and professor Daniel Galaviz for kindly receiving me and making me feel part of the team, as well as for everything that I have learned in this internship with them.

References

[1] P. Shukla, S. Sankrith, International Journal of Modern Physics A **33**, 1850175 (2018)

[2] C. Schwerdt, Wissenschaftliche Koordinatorin Cosmic-Projekte, Zeuthen. Web sitesi: https://icd. desy. de/sites/sites_conferences/site_icd/content/e12688/e13082/e80711/Cosmic@ Web_engl. pdf. Erişim Tarihi **21** (2018)

[3] G.F. Knoll, *Radiation detection and measurement* (John Wiley & Sons, 2010)

[4] D.E. Groom, N.V. Mokhov, S.I. Striganov, Atomic Data and Nuclear Data Tables **78**, 183 (2001)

[5] D.E. Groom, S. Klein, The European Physical Journal C-Particles and Fields **15**, 163 (2000)

[6] L.J. Schultz, G.S. Blanpied, K.N. Borozdin, A.M. Fraser, N.W. Hengartner, A.V. Klimenko, C.L. Morris, C. Orum, M.J. Sossong, IEEE Transactions on Image Processing **16**, 1985 (2007)

[7] A. Souza, A. Massafferri, A. Neto, E. Pereyra, F. Sousa, G. Alves, G. Oliveira, J. Marcolan, P. Sardelich, V. Cunha et al., Notas Técnicas **8**, 25 (2018)

[8] ET-Enterprises, *9814b series data sheet*, https://et-enterprises.com/images/data_sheets/9814B.pdf

[9] T.M.I. Revision, *Introduction to topas*, https://topas.readthedocs.io/en/latest/getting-started/intro.html

[10] T.M.I. Revision, *Introduction to scorers*, https://topas.readthedocs.io/en/latest/parameters/scoring/intro.html

[11] T. nBio Collaboration Revision, *Introduction to topas-nbio*, https://nbio.readthedocs.io/en/latest/getting-started/Introduction.html

[12] C. Hagmann, D. Lange, D. Wright, *Cosmic-ray shower generator (CRY) for Monte Carlo transport codes*, in *2007 IEEE Nuclear Science Symposium Conference Record* (2007), Vol. 2, pp. 1143–1146

[13] G. Collaboration, *About geant4*, https://geant4.web.cern.ch/about/

A Information given by scorers in TOPAS

A.1 Phase Space scorers information

The phase space scorers in TOPAS give: Position (x,y,z) [cm], Direction Cosine in x and y, Energy [MeV], weight, Type (in PDG Format), Flag to tell if third Direction Cosine is negative (1 means true), Flag to tell if it is the First Scored Particle from this History (1 means true), Run ID, Event ID and Track ID od each particle.

A.2 TOPAS-nBio scorers information

The TOPAS-nBio scorers give: Molecule ID or Particle PDG, Position (x,y,z) [um], Event ID, Track ID, Step number, Particle name, Process name, Volume name, Volume copy number, Parent A ID, Parent B ID, Vertex position (x,y,z) [um], Global time (ps), Energy deposited [keV] and Kinetic energy [keV].

B TOPAS code

Here the code for the TOPAS setup as well as for the phase space and nBio scorers can be found.

C Python Code

C.1 Data Analysis

Here the codes for the different scorers output analysis can be found.

- Phase Space Scorer
- nBio Scorer
- CRY-TOPAS Scorer

C.2 CRY to TOPAS

Here the code that transposes the CRY output to a TOPAS input can be found.

D Geant4 code

Here the codes for the energy deposited can be found.

E DataSheets

Here, one can find the links that direct to the data sheets of the materials used in this project.

Power Supply
Photomultiplier Tube
EJ-200 Scintillator
Oscilloscope